IET Radar, Sonar & Navigation

Research Article

IET Journals
The Institution of Engineering and Technology

Robust variability index CFAR for non-homogeneous background

ISSN 1751-8784
Received on 24th September 2018
Revised 23rd May 2019
Accepted on 3rd June 2019
E-First on 16th July 2019
doi: 10.1049/iet-rsn.2018.5435
www.ietdl.org

Narasimhan Raman Subramanyan[1] ✉, Ramakrishnan Kalpathi R.[1], Vengadarajan A.[2]

[1]*Department of Electrical Engineering, Indian Institute of Science, Bangalore, India*
[2]*DRDO, Ministry of Defence, Bangalore, India*
✉ *E-mail: narasimhanrs80@gmail.com*

Abstract: Radar signal detection using constant false alarm rate (CFAR) detectors encounters many non-ideal situations making it difficult to characterise the background. These include the presence of multiple targets, clutter edges and their combination in the reference window. Designing an efficient CFAR for these situations is a non-trivial problem. Algorithms based on ordered statistics (OS), outlier rejection using sorting and sample by sample hypothesis testing, variability index (VI), ordered data VI are proposed in the literature. These approaches require expensive sorting or prior information on the depth of censoring. In this study, the authors propose robust VI CFAR (RVI-CFAR) that obviates sorting. RVI-CFAR computes the threshold in multiple stages. The first stage uses VI-CFAR to determine an adaptive threshold. Outlier rejection in the computation of background, mean ratio (MR) and VI is carried out in subsequent stages. The updated MR and VI statistics are used to refine switching decisions at every stage of processing. RVI-CFAR exhibits low CFAR loss in homogeneous and multiple target scenarios, meanwhile achieving superior performance compared to other censored CFAR techniques. The proposed RVI-CFAR is evaluated and shown to be robust for all the cases of non-homogeneity compared to OS CFAR.

1 Introduction

Target detection at a given range cell is a hypothesis testing problem with two hypotheses namely, null hypothesis, which represents the interference only condition, and alternate hypothesis representing the target return plus interference. A target is declared at a given range cell if the strength of the return exceeds a given threshold. The threshold is determined by solving a constrained optimisation problem, which maximises the target detection probability for a given probability of false alarm (PFA). In practice, such fixed threshold detectors fail to maintain a constant false alarm rate (CFAR) due to varying interference characteristics. Adaptive threshold detectors are used to detect radar signals with varying interference power while maintaining CFAR. Hence, such detectors are called 'CFAR' detectors. In CFAR processing, the interference power is estimated from signal samples (also called training samples) and this estimate is used to set the threshold. The signal samples used for background estimation are called reference or secondary samples. The decision range cell is referred to as 'cell under test' (CUT). The threshold is fixed based on statistical characteristics of the reference samples to maintain false leaks out of the detector at the desired level. The statistical characteristics of interference at the test cell are assumed to be identical to reference cells. This is usually true if the considered reference range cells are neighbouring range cells of the test cell. One of the computationally light and most popular CFAR detectors is 'cell-averaging' CFAR (CA-CFAR) [1]. CA-CFAR is suitable for target detection under homogeneous background. The condition of homogeneity is an ideal situation and is violated very often resulting in the sub-optimum performance of CA-CFAR. The contamination of the reference window of the test cell due to signal returns from other targets is a very common scenario. This inhibits the accurate estimation of the interference power level. In this study, targets appearing in the secondary cells of the test cell (CUT) are classified as outliers for the background estimation problem. Strong target returns present in the reference window could severely degrade the detection performance of target under consideration, which is hereafter called 'primary target' (target in test cell). This effect is referred to as 'capture effect'. We evaluate the proposed CFAR technique for the following scenarios of background interference, which are the main causes for the lack of homogeneity in the background data:

i. *Multiple target environments:* This condition is characterised by the presence of signal returns from other targets in the reference window of the cell under test. This violates the assumption that the samples in secondary range cells are drawn from an independent and identical distribution (i.i.d). This leads to masking of the primary target.
ii. *Clutter edge environment:* This condition is characterised by the abrupt change in interference power from a lower level to a higher level or vice-versa within the reference window. The presence of clutter edge has two effects. It sets the threshold higher for test cells in the clear region, thereby masking the weaker targets. Also, the threshold is set lower for test cells in the higher clutter region resulting in intolerable false leaks. In this study, we assume a single clutter transition from low to high when traversed from left to right along the range axis.
iii. *Combination of clutter edge and interfering targets:* In this condition, the reference window contains a clutter edge and multiple interfering targets.

Variants of computationally light CA-CFAR technique have been studied and proposed in the literature to address the non-homogeneous background scenarios. 'Smallest-of' CFAR (SO-CFAR) [2] and 'greater of' CFAR (GO-CFAR) [3, 4] are variants of CA-CFAR. SO-CFAR addresses the target masking effect caused by interfering targets situated on one side of the test cell but fails to contain false leaks at a clutter edge. On the other hand, GO-CFAR regulates false leaks at the clutter edge, but the detector's performance severely degrades in multiple target environments. A good discussion on CA-CFAR and its variants under non-homogeneous scenario can be found in [5, 6]. In [7], the authors propose an iterative procedure to exclude samples exceeding an adaptive threshold from the reference set. Iterative censoring of outlier samples for target detection in synthetic-aperture radar (SAR) images is proposed in [8]. Censoring of outliers based on the global threshold is proposed in [9]. However, these techniques do not address the non-homogeneity caused by clutter edges and a combination of clutter edge and interfering targets. In [10],

'switching censored cell averaging greater of (SCCAGO)' CFAR detector is proposed to handle both multiple interfering target scenarios and clutter edge independently, but the detector fails to handle scenarios where the reference window contains both clutter edge and interfering targets.

'Ordered statistics' CFAR (OS-CFAR) [11] is proposed to alleviate the problem of target masking in a multiple target environment but the detector is not very effective in regulating excessive false leaks at clutter edge [12]. OS-CFAR chooses a certain signal sample from the sorted sequence as background estimate and the position of this sample determines the depth of censoring. The optimum depth of censoring for a given scenario requires the knowledge of the expected number of interfering targets, which is generally not known a-priori. Furthermore, the need for sorting makes the implementation complex. Switched OS CFAR is proposed in [13] and trimmed mean (TM) CFAR [14–17] are modified versions of OS-CFAR proposed to improve the performance of OS-CFAR at the clutter edge and multiple target scenarios. The performance of TM-CFAR degrades more gracefully, unlike OS-CFAR in the presence of more interfering targets than the number of censored samples. To address the practical difficulty of choosing the depth of censoring in OS-CFAR and its variants, detectors based on a sample by sample hypothesis testing on the sorted sequence are proposed in the literature. Generalised censored mean level detector [16], automatic censored greater of CFAR [18, 19], GO/SO-CFAR detector [20], automatic censored mean level detector CFAR [20] and generalised two-level censored mean level detector [20] belong to this category of detectors. All these detectors require sorting followed by sample by sample hypothesis testing and thus are computationally expensive. Automatic censored cell averaging CFAR (CA-CFAR) is proposed in [21], which performs cell by cell test to censor unwanted samples without the need to rank the samples and is designed to handle multiple clutter transitions in the reference window. The disadvantage of this approach is that it handles non-homogeneity caused due to clutter edges only. Furthermore, the sample support considered for background estimation is not optimum. In [16], a weighted CA-CFAR technique is proposed. In [22], a CFAR detector with truncated statistics is proposed. 'Cell averaging TM' CFAR, 'cell averaging ordered statistics (OS)' CFAR are other CFAR detectors proposed in the literature to improve the performance for non-homogeneous background [23]. An extension of TM-CFAR method is proposed in [24]. An intelligent CFAR detector called, 'variability index' CFAR (VI-CFAR) is proposed in [25]. The performance of VI-CFAR degrades severely if the interfering targets are distributed on either side of the test cell. This is the major limitation of VI-CFAR. The performance of VI-CFAR for marine target detection under non-homogeneous background is presented in [26]. In [27], the performance of VI-CFAR is improved using fuzzy techniques for simple cases of non-homogeneity. In [28], the VI is computed on the ordered set of samples to determine the depth of censoring. The CFAR scheme is called automatic censored cell averaging CFAR based on ordered data VI. This approach requires an expensive sorting operation to be performed. In addition, the size of the initial population considered to represent the background estimate is very critical to achieve desired performance and this need to be chosen a-priori. A CFAR detector based on ordered data variability is proposed in [29]. Variations of VI-CFAR using OS is proposed in [30–33]. A dual threshold robust CFAR method is proposed in [34]. CFAR methods based on neural networks are discussed in [35]. Outlier identification and rejection based on Grubbs criterion is proposed in [36].

In this study, we propose an efficient robust VI CFAR (RVI-CFAR) for complex scenarios with both interfering targets and clutter edge in the reference window. The proposed RVI-CFAR is an improved version of detectors proposed in our previous work [10]. RVI-CFAR does not require sorting operation for outlier rejection from training samples and thus it is computationally efficient. In addition, RVI-CFAR exhibits robust detection performance in the presence of clutter edge and multiple interfering targets in the training data or reference window. Besides this, RVI-CFAR detector also minimises the CFAR loss compared to other censored CFAR techniques by selectively removing the extraneous samples from the training data. The outlier identification and rejection is carried out in multiple stages. At any stage of processing, outliers are those signal samples which exceed the computed local threshold at that stage. RVI-CFAR obviates the issues associated with other CFAR schemes viz., the decision on the depth of censoring, the decision on optimum reference window size, performance degradation due to higher CFAR loss, cell by cell hypothesis testing to reject or accept a sample. Additionally, RVI-CFAR avoids the sorting of samples for outlier rejection. RVI-CFAR is evaluated for clutter edge and multiple interfering target scenarios and its performance is compared with other CFAR techniques (VI, OS CFAR schemes). The evaluation is carried out for homogeneous, multiple targets (scenario I), clutter edge (scenario II) and combination of interfering targets and clutter edge (scenario III) cases.

2 Variability index CFAR (VI-CFAR)

2.1 Radar signal model

The radar under consideration uses digital down conversion producing in-phase and quadrature-phase (I/Q) signal samples. The statistical distribution of interference or noise samples in I/Q channels obey Gaussian distribution and are independent and identically distributed with zero mean. CFAR is performed on the signal samples, which are magnitude square of samples from I/Q channels. The magnitude square of complex white Gaussian random variable with zero mean is exponentially distributed [37] and is given by

$$f_X(x) = \frac{1}{\lambda} e^{(-(1/\lambda)x)} x \geq 0, \quad \lambda > 0. \tag{1}$$

The null hypothesis H_0 models interference and the alternate hypothesis H_1 models target return plus interference. Thus, under hypothesis H_0, the observation samples are exponentially distributed given by (1) with parameter μ. This is the background interference power. In this study, it is assumed that the target radar cross section follows Swerling-1 model and hence the signal-to-noise ratio (SNR) of target return signal follows an exponential distribution. Under hypothesis H_1, the signal samples are governed by exponential probability density function with parameter $\mu(1 + S)$, where S is the average SNR of the Swerling-1 target. The value of parameter λ under different hypotheses is given by

$$\lambda = \begin{cases} \mu, & \text{under no target condition,} \\ \mu(1+S), & \text{under target condition .} \end{cases}$$

The radar considered here is a pulse Doppler radar capable of measuring range and Doppler of targets of interest. To achieve this, the radar uses a coherent processing interval consisting of multiple transmission pulses. The signal conditioning operations such as pulse compression, clutter filtering and coherent processing (also called moving target discrimination) are performed before CFAR operation. The CFAR is performed along the range axis for every Doppler filter on a range-Doppler map generated as a result of signal processing operations. In this study, we have described the design of RVI-CFAR detector for a given Doppler filter along range direction.

2.2 Description of VI-CFAR

CA-CFAR is suitable for homogeneous background, whereas SO and GO-CFAR detectors are more appropriate for interfering target and clutter edge scenarios, respectively. The CA-CFAR utilises $2N$ signal samples surrounding the test cell (i.e. CUT) to estimate background interference power. Here, $2N$ is the sample support or the number of training samples. In CA-CFAR, threshold multiplier α is computed as in (2) for the reference window size of $2N$ and given mean PFA $\bar{P}_{\mathrm{FA}}$ [38]. Since GO/SO CFAR detectors use half reference window for background estimation value of N is used in (2) to compute threshold multiplier α.

A dynamically changing background requires the CFAR scheme to be switched between CA, SO and GO CFAR detectors to adapt to the type of outlier present in the reference samples. VI-CFAR [25] provides a method to choose the CFAR detector best suited for a given scenario. VI-CFAR achieves this by computing the first-order statistics called mean ratio (MR) between the right and the left reference windows and the second-order statistics called VI of the right and left reference windows. The outcome of hypothesis tests conducted on MR and VI values at a given test cell chooses either right or left or both neighbours of the test cell for background estimation. Let L be the total number of range cells in a given Doppler filter. The signal samples corresponding to L range cells are denoted by $x_1, x_2, x_3, \ldots, x_L$ in the order of sampling time. Given a range cell r_j, the right neighbours (lagging reference window) are $r_j + G + 1$ to $r_j + N + G$ and the left neighbours (leading reference window) are the range cells $r_j - N - G$ to $r_j - G - 1$, where G is the number of guard cells and $2N$ is the size of the reference window. Generally, guard cells are considered to exclude the leakage of the target return signal, present in a cell under test, from background estimate

$$\alpha = 2N(\bar{P}_{\mathrm{FA}}^{-1/2N} - 1). \tag{2}$$

The following sets are defined with the assumption $L > 2N + 2G + 1$.

Left neighbours of test cell j

$$\mathscr{N}_j^{\mathrm{l}} = \begin{cases} \{j - N - G, \ldots, j - G - 1\}, & \forall j \in \mathscr{Z}_l, \\ \{1, \ldots, j - G - 1\}, & G + 1 < j < N + G + 1, \\ \{\phi\}, & \text{otherwise}, \end{cases}$$

where $\mathscr{Z}_l = \{N + G + 1, \ldots, L\}$ denotes an integer set.

Right neighbours of test cell j

$$\mathscr{N}_j^{\mathrm{r}} = \begin{cases} \{j + G + 1, \ldots, j + N + G\}, & \forall j \in \mathscr{Z}_r, \\ \{j + G + 1, \ldots, L\}, & L - N - G < j < L - G, \\ \{\phi\}, & \text{otherwise}, \end{cases}$$

where $\mathscr{Z}_{\mathrm{r}} = \{1, \ldots, L - N - G\}$ denotes an integer set.

Two sided neighbours of test cell i

$$\mathscr{N}_j = \mathscr{N}_j^{\mathrm{l}} \cup \mathscr{N}_j^{\mathrm{r}}. \tag{3}$$

Range sample vector $\boldsymbol{r}$

$$\boldsymbol{r} = [x_1 x_2 \ldots x_L].$$

For a given test cell j, VI and mean of right and left windows are given by

VI of the right (lagging) window

$$\mathrm{VI}_j^{\mathrm{r}} = 1 + \frac{1}{\left|\mathscr{N}_j^{\mathrm{r}}\right| - 1} \frac{\sum_{k \in \mathscr{N}_j^{\mathrm{r}}} (x_k - \overline{X}_j^{\mathrm{r}})^2}{(\overline{X}_j^{\mathrm{r}})^2}.$$

VI of the left (leading) window

$$\mathrm{VI}_j^{\mathrm{l}} = 1 + \frac{1}{\left|\mathscr{N}_j^{\mathrm{l}}\right| - 1} \frac{\sum_{k \in \mathscr{N}_j^{\mathrm{l}}} (x_k - \overline{X}_j^{\mathrm{l}})^2}{(\overline{X}_j^{\mathrm{l}})^2}.$$

Mean of the right (lagging) window

$$\overline{X}_j^{\mathrm{r}} = \frac{1}{\left|\mathscr{N}_j^{\mathrm{r}}\right|} \sum_{k \in \mathscr{N}_j^{\mathrm{r}}} x_k.$$

Mean of the left (leading) window

$$\overline{X}_j^{\mathrm{l}} = \frac{1}{\left|\mathscr{N}_j^{\mathrm{l}}\right|} \sum_{k \in \mathscr{N}_j^{\mathrm{l}}} x_k.$$

The MR is defined as

$$\mathrm{MR}_j = \frac{\overline{X}_j^{\mathrm{l}}}{\overline{X}_j^{\mathrm{r}}}.$$

The VI-CFAR employs a suitable CFAR detector from CA, SO and GO CFAR detectors based on the outcome of hypothesis tests performed on VI and MR at any given test cell. The algorithm uses thresholds on MR and VI to perform hypothesis testing. The threshold value of VI is denoted by K_{VI} and the threshold used for the MR hypothesis test is denoted by K_{MR}. To determine whether the training samples form homogeneous background or otherwise, the VI-CFAR detector compares the VI value computed from these samples with the threshold K_{VI} through the hypothesis test indicated in (4). Equation (4) shows the hypothesis test for the left-side window. Similar to this, the test is conducted for the right-side window as well

$$\begin{aligned} &\mathrm{VI}_j^{\mathrm{l}} \le K_{\mathrm{VI}} \Rightarrow \text{homogeneous}, \\ &\mathrm{VI}_j^{\mathrm{l}} > K_{\mathrm{VI}} \Rightarrow \text{non} - \text{homogeneous}. \end{aligned} \tag{4}$$

The MR value is compared against the threshold K_{MR} to determine whether the mean of right and left reference windows are similar or dissimilar as depicted in (5)

$$\begin{aligned} &K_{\mathrm{MR}}^{-1} \le \mathrm{MR}_j \le K_{\mathrm{MR}} \Rightarrow \text{same mean}, \\ &\mathrm{MR}_j < K_{\mathrm{MR}}^{-1} \text{ or } \mathrm{MR}_j > K_{\mathrm{MR}} \Rightarrow \text{different mean}. \end{aligned} \tag{5}$$

The CFAR switching policy adopted in VI-CFAR is stated in Table 1. As clutter samples start entering the reference window from the right, the right half will be non-homogeneous initially (due to one or two samples from the clutter region and rest from the thermal noise region), whereas the left window will be homogeneous. This situation corresponds to the third row of Table 1 and CA-CFAR with samples from the left window is used to compute the threshold. As clutter samples fill up the right window, both the reference windows will appear homogeneous with different means and the selection algorithm will choose the window with higher mean to contain false leaks. This is indicated by the first row in Table 1. As the clutter samples start populating the left window, the left window will be non-homogeneous, whereas the right window will be homogeneous. This situation corresponds to the fourth row in Table 1 and only the right samples (higher power region) are used for background estimation. Finally, as clutter samples fill up both the windows, each will appear homogeneous and combined window will be selected. However, VI-CFAR switching policy is not ideal for multiple target scenarios. In this study, we propose an improved version of VI-CFAR called 'RVI-CFAR'. The performance of VI-CFAR degrades if both clutter edge and interfering targets appear in the reference window of the cell under test. We propose to solve this situation using RVI-CFAR detector.

3 Robust VI-CFAR

The VI-CFAR introduced in Section 2 suffers from severe loss in performance if the reference window contains other targets on either side of the test cell. Furthermore, the presence of non-homogeneity (either interfering targets or clutter edge) on both sides of the test cell is not addressed by VI-CFAR. In this section, we propose RVI-CFAR to address this scenario in a

Table 1 CFAR switching rule for VI CFAR detector

Case	Is left window homogeneous	Is right window homogeneous	Is mean different	CFAR scheme	Adaptive threshold
1	yes	yes	yes	GO CFAR	$\alpha_N \cdot \max(\overline{X}^{\mathrm{l}}, \overline{X}^{\mathrm{r}})$
2	yes	yes	no	CA CFAR	$\alpha_{2N} \cdot \overline{X}^{\mathrm{lr}}$
3	yes	no	—	CA CFAR	$\alpha_N \cdot \overline{X}^{\mathrm{l}}$
4	no	yes	—	CA CFAR	$\alpha_N \cdot \overline{X}^{\mathrm{r}}$
5	no	no	—	SO CFAR	$\alpha_N \cdot \min(\overline{X}^{\mathrm{l}}, \overline{X}^{\mathrm{r}})$

computationally efficient manner. The proposed RVI-CFAR detector does not rely on sorting of power returns in the reference window to identify and reject outliers, which is the salient feature of the detector.

The first stage of RVI-CFAR computes the detection threshold using the standard VI-CFAR detector. The second stage considers the range samples, which exceed the set threshold determined by VI-CFAR, in the first stage, as outliers and excludes them from background estimate and VI and MR statistics. The outlier rejection is carried out on a small subset of total range samples, which are formed by the detected range cells in the first stage and all their neighbours or reference cells. Let us assume that P cells out of L cross the VI-CFAR threshold in the first stage. Generally, in radar applications, the PFA is set low and hence $P \ll L$. Let $x_{r_1}, x_{r_2}, \ldots x_{r_P}$ represent signal samples of the detected set of range cells $\{r_1, r_2, \ldots, r_P\}$ from the first stage. In the second stage, outliers detected (or targets detected) in the first stage are censored. The outlier rejection from background estimation and VI and MR statistics facilitates the detection of new targets in the second stage, which are otherwise masked by the presence of strong signal returns from interfering targets in their reference window.

The CFAR threshold is fixed to achieve the design level of PFA and this is referred to as 'detection threshold'. An improvement in the performance of the RVI-CFAR detector is possible if a different threshold, lesser than the detection threshold, is used for identification of outliers in the training samples. This threshold is referred to as 'outlier detection threshold'. This threshold can be fixed to identify extraneous samples of low SNR. Too low a threshold for outlier detection has two adverse impacts; (a) it increases the computational load, (b) it starts censoring even the noise samples at very low thresholds, thereby reducing the number of samples available for background estimation (amounting to higher CFAR loss). A careful choice of this threshold can enhance the performance of censored CFAR detectors. The PFA corresponding to outlier detection threshold can also be considered as the probability of false censoring (PFC) $\tilde{P}_{\mathrm{FC}}$.

In RVI-CFAR, the adaptive threshold is determined based on the outcomes of the hypothesis tests performed on VI and MR and the adopted switching policy is identical to VI-CFAR as summarised in Table 1. The computation of background sum vector $\boldsymbol{b}$ and sample support vector $\boldsymbol{w}$ depends on the neighbourhood definition. For a given test cell j either half window or full window is considered as neighbours, based on the CFAR switching rule. The local neighbours (alternatively reference window) of j, $\mathcal{N}_j^{\mathrm{S}}$, under RVI-CFAR detector is given in (6).

$$\mathcal{N}_j^{\mathrm{S}} = \begin{cases} \mathcal{N}_j, & \text{if case} - 2, \\ \mathcal{N}_j^{\mathrm{l}}, & \text{if case} - 1 \text{ with } \mathrm{MR}_j \geq 1, \\ \mathcal{N}_j^{\mathrm{r}}, & \text{if case} - 1 \text{ with } \mathrm{MR}_j < 1, \\ \mathcal{N}_j^{\mathrm{l}}, & \text{if case} - 3, \\ \mathcal{N}_j^{\mathrm{r}}, & \text{if case} - 4, \\ \mathcal{N}_j^{\mathrm{l}}, & \text{if case} - 5 \text{ with } \mathrm{MR}_j \leq 1, \\ \mathcal{N}_j^{\mathrm{r}}, & \text{if case} - 5 \text{ with } \mathrm{MR}_j > 1. \end{cases} \tag{6}$$

The background sum vector $\boldsymbol{b}$, sample support vector $\boldsymbol{w}$ and threshold vector $\boldsymbol{t}^{\mathrm{D}}$ are computed as given in (7), (8) and (9) applying neighbourhood definition as shown in (6).

The background sum vector $\boldsymbol{b}$ is modified based on the CFAR method and its jth column entry is given by

$$\boldsymbol{b}_j = \sum_{k \in \mathcal{N}_j^{\mathrm{S}}} x_k \text{ or } \sum_{k \in \mathcal{N}_j^{\mathrm{S}}} \boldsymbol{r}_k, \tag{7}$$

where $\boldsymbol{r}_k$ is the kth column of $\boldsymbol{r}$.

Sample support vector $\boldsymbol{w}$ with the jth column entry is given by

$$\boldsymbol{w}_j = \left|\mathcal{N}_j^{\mathrm{S}}\right|, \tag{8}$$

where $\left|\mathcal{N}_j^{\mathrm{S}}\right|$ is the cardinality of set $\mathcal{N}_j^{\mathrm{S}}$.

Final detection threshold vector $\boldsymbol{t}^{\mathrm{D}}$ with the jth column entry is given by

$$\boldsymbol{t}_j^{\mathrm{D}} = \alpha_j^{\mathrm{D}} \frac{1}{\boldsymbol{w}_j} \boldsymbol{b}_j, \tag{9}$$

The cardinality of the set $\mathcal{N}_j^{\mathrm{S}}$ (or $\boldsymbol{w}_j$) is substituted in (2) along with design $\tilde{P}_{\mathrm{FA}}$ to determine α_j^{D}.

Outlier detection threshold vector $\boldsymbol{t}^{\mathrm{O}}$ with the jth column entry is given by

$$\boldsymbol{t}_j^{\mathrm{O}} = \alpha_j^{\mathrm{O}} \frac{1}{\boldsymbol{w}_j} \boldsymbol{b}_j. \tag{10}$$

The cardinality of the set $\mathcal{N}_j^{\mathrm{S}}$ (or $\boldsymbol{w}_j$) is substituted in (2) along with design $\tilde{P}_{\mathrm{FC}}$ to determine α_j^{O}.

Final detection vector $\boldsymbol{d}^{\mathrm{D}}$ with the jth column entry

$$\boldsymbol{d}_j^{\mathrm{D}} = \begin{cases} 1, & \boldsymbol{r}_j \geq \boldsymbol{t}_j^{\mathrm{D}}, \\ 0, & \text{otherwise}. \end{cases}$$

Outlier detection vector $\boldsymbol{d}^{\mathrm{O}}$ with the jth column entry

$$\boldsymbol{d}_j^{\mathrm{O}} = \begin{cases} 1, & \boldsymbol{r}_j \geq \boldsymbol{t}_j^{\mathrm{O}}, \\ 0, & \text{otherwise}. \end{cases}$$

The second stage of the RVI-CFAR detector considers the detected range cells from the first stage as outliers and removes their contribution from the background estimate, VI and the MR of all the affected range cells. The requisite information on the type of CFAR and corresponding neighbourhood considered for all range cells in the first stage and subsequent stages is maintained to facilitate censoring operation. To reduce the computational requirement, we use the simplified VI statistic (biased maximum likelihood estimate) as defined in [25] and reproduced here in (11)

$$VI_j^{*\mathrm{l}} = \left|\mathcal{N}_j^{\mathrm{l}}\right| \frac{\sum_{k \in \mathcal{N}_j^{\mathrm{l}}} (x_k)^2}{\left(\sum_{k \in \mathcal{N}_j^{\mathrm{l}}} x_k\right)^2} = \boldsymbol{w}_j^{\mathrm{l}} \frac{\boldsymbol{s}_j^{\mathrm{l}}}{\left(\boldsymbol{f}_j^{\mathrm{l}}\right)^2}, \tag{11}$$

where $\boldsymbol{w}_j^{\mathrm{l}}$ is the cardinality of set $\mathcal{N}_j^{\mathrm{l}}$, $\boldsymbol{s}_j^{\mathrm{l}}$ is the sum of squares of samples in the left reference window of range cell j and $\boldsymbol{f}_j^{\mathrm{l}}$ is the sum of samples in the left reference window of range cell j. We define the following vectors.

Left sample support vector $\boldsymbol{w}^{\mathrm{l}}$ with the jth column (corresponding to jth range cell) as

$$\boldsymbol{w}_j^{\mathrm{l}} = \left|\mathcal{N}_j^{\mathrm{l}}\right|, \quad \text{for } j1 \text{ to } L.$$

Similarly, right sample support vector $\boldsymbol{w}_j^{\mathrm{r}}$ with the jth column is given by

$$\boldsymbol{w}_j^{\mathrm{r}} = \left|\mathcal{N}_j^{\mathrm{r}}\right|, \quad \text{for } j\,1 \text{ to } L.$$

Left background sum vector $\boldsymbol{f}^{\mathrm{l}}$ with the jth column (corresponding to jth range cell) as

$$\boldsymbol{f}_j^{\mathrm{l}} = \sum_{k \in \mathcal{N}_j^{\mathrm{l}}} x_k, \quad \text{for } j\,1 \text{ to } L.$$

Similarly, right background sum vector $\boldsymbol{f}^{\mathrm{r}}$ with the jth column is given by

$$\boldsymbol{f}_j^{\mathrm{r}} = \sum_{k \in \mathcal{N}_j^{\mathrm{r}}} x_k, \quad \text{for } j\,1 \text{ to } L.$$

The sum of squares of left samples vector $\boldsymbol{s}^{\mathrm{l}}$ with the jth column (corresponding to the jth range cell) as

$$\boldsymbol{s}_j^{\mathrm{l}} = \sum_{k \in \mathcal{N}_j^{\mathrm{l}}} (x_k)^2, \quad \text{for } j\,1 \text{ to } L.$$

Similarly, the sum of squares of right samples vector $\boldsymbol{s}^{\mathrm{r}}$ with the jth column is given by

$$\boldsymbol{s}_j^{\mathrm{r}} = \sum_{k \in \mathcal{N}_j^{\mathrm{r}}} (x_k)^2, \quad \text{for } j\,1 \text{ to } L.$$

At the beginning of every iteration of outlier removal, all the vectors $\boldsymbol{b}' = \boldsymbol{b}$, $\boldsymbol{w}' = \boldsymbol{w}$, $\boldsymbol{w}'^{\mathrm{l}} = \boldsymbol{w}^{\mathrm{l}}$, $\boldsymbol{w}'^{\mathrm{r}} = \boldsymbol{w}^{\mathrm{r}}$, $\boldsymbol{s}'^{\mathrm{l}} = \boldsymbol{s}^{\mathrm{l}}$, $\boldsymbol{s}'^{\mathrm{r}} = \boldsymbol{s}^{\mathrm{r}}$, $\boldsymbol{f}'^{\mathrm{l}} = \boldsymbol{f}^{\mathrm{l}}$, and $\boldsymbol{f}'^{\mathrm{r}} = \boldsymbol{f}^{\mathrm{r}}$ are initialised. The censoring algorithm has two major steps and they are

- Identification of outliers [10].
- Censoring of outliers.

3.1 Identification of outliers

Given outlier detection vector $\boldsymbol{d}^{\mathrm{O}}$ and range sample vector $\boldsymbol{r}$, the identification of outliers involves the following steps:

- Inputs:
  - $\boldsymbol{r} \in \mathbb{R}^{1\times L}$ – range sample vector
  - $\boldsymbol{d}^{\mathrm{O}} \in \mathbb{R}^{1\times L}$ – outlier detection vector
- Output:
  - Detected range cells (outliers) grouped into set $\mathcal{M}_r$

The algorithm proceeds as follows:

i. If guard cells are considered then –
   - Compute $\boldsymbol{r}' = \boldsymbol{d}^{\mathrm{O}} \circ \boldsymbol{r}$, where $\circ$ denotes the Hadamard product.
   - Compute $\boldsymbol{r}^d = \Delta \boldsymbol{r}'$, where Δ denotes difference operator of first order defined as $\boldsymbol{r}_j^d = \boldsymbol{r}_i' - \boldsymbol{r}_{i-1}'$.
   - Augmented vector is formed as $\boldsymbol{r}^{dA} = [0\boldsymbol{r}^d]$.
   - The range cell, which is local maxima is located as
     - Compute $\boldsymbol{s}_{\boldsymbol{r}^{dA}} = \mathrm{sign}(\boldsymbol{r}^{dA})$, where the function sign(·) returns the sign of vector elements. It returns 1 if the element is positive, −1 if negative and 0 if zero.
     - Compute $\boldsymbol{s}^d = [\Delta \boldsymbol{s}_{\boldsymbol{r}^{dA}} 0]$.
     - The location of local maxima of range samples is given by the column position in the vector $\boldsymbol{s}^d$ with the entry −2 or 2

$$\mathcal{M}_r = \{j : \boldsymbol{s}_j^d = \pm 2\}.$$

ii. If guard cells are not considered –

$$\mathcal{M}_r = \{j : \boldsymbol{d}_j^{\mathrm{O}} = 1\}.$$

iii. Let P be the cardinality of set $\mathcal{M}_r$ and $r_{\max 1}, r_{\max 2}, \ldots, r_{\max P}$ be the positions of local maxima. These correspond to detected range cell positions with peak strength at any stage of processing.

3.2 Censoring of outliers

As the values of VI and MR are sensitive to the presence of outliers and their values decide the outcome of hypothesis tests, thereby dictating the adaptive threshold, censoring of outliers in the computation of VI and MR is imperative to arrive at the appropriate CFAR method. The outlier rejection step is described here considering every detected range cell $r_{\max i} \in M_r$ and has the following sub-steps:

- $\forall\, r_{\max i} \in \mathcal{M}_r$ and its guard cells, $r_{\max i} - 2$, $r_{\max i} - 1$, $r_{\max i} + 1$ and $r_{\max i} + 2$ (if considered) perform the following :
  - Update MR of neighbours of range cell $r_{\max i}$:

The MR is recomputed to exclude the detected range cell. The sum of samples from the right window of all left neighbours of the detected range cell is updated omitting the detected range cell as an outlier. Similarly, the sum of samples from the left window of all right neighbours of the detected range cell is also recomputed excluding the detected range.

Update sum of left window and left sample support corresponding to right neighbours of $r_{\max i}$

$$\forall j \in \mathcal{N}_{r_{\max i}}^{\mathrm{r}}, \quad \boldsymbol{f}'^{\mathrm{l}}_j = \boldsymbol{f}'^{\mathrm{l}}_j - x_{r\max i}, \quad \boldsymbol{w}'^{\mathrm{l}}_j = \boldsymbol{w}'^{\mathrm{l}}_j - 1. \tag{12}$$

Update sum of right window and right sample support corresponding to left neighbours of $r_{\max i}$

$$\forall j \in \mathcal{N}_{r_{\max i}}^{\mathrm{l}}, \quad \boldsymbol{f}'^{\mathrm{r}}_j = \boldsymbol{f}'^{\mathrm{r}}_j - x_{r_{\max i}}, \quad \boldsymbol{w}'^{\mathrm{r}}_j = \boldsymbol{w}'^{\mathrm{r}}_j - 1. \tag{13}$$

Update MR of all the neighbours of $r_{\max i}$:

$$\forall j \in \mathcal{N}_{r_{\max i}}, \quad \mathrm{MR}_j = \frac{\boldsymbol{w}'^{\mathrm{r}}_j \boldsymbol{f}'^{\mathrm{l}}_j}{\boldsymbol{w}'^{\mathrm{l}}_j \boldsymbol{f}'^{\mathrm{r}}_j}. \tag{14}$$

- Update VI of all the neighbours of $r_{\max i}$:

The right VI of all left neighbours of detected range cell is updated omitting the detected range cell as an outlier. Similarly, the left VI of all right neighbours of detected range cell is also recomputed excluding the outlier.

Update sum of squares of samples from the left window corresponding to right neighbours of $r_{\max i}$

$$\forall j \in \mathcal{N}_{r_{\max i}}^{\mathrm{r}}, \quad \boldsymbol{s}'^{\mathrm{l}}_j = \boldsymbol{s}'^{\mathrm{l}}_j - \left(x_{r_{\max i}}\right)^2. \tag{15}$$

Update sum of squares of samples from the right window corresponding to left neighbours of $r_{\max i}$:

$$\forall j \in \mathcal{N}^{\mathrm{l}}_{r_{\mathrm{max}i}}, \quad \boldsymbol{s}'^{\mathrm{r}}_j = \boldsymbol{s}'^{\mathrm{r}}_j - \left(x_{r_{\mathrm{max}i}}\right)^2. \tag{16}$$

Update right VI of left neighbours of $r_{\mathrm{max}i}$

$$\forall j \in \mathcal{N}^{\mathrm{l}}_{r_{\mathrm{max}i}}, \quad \mathrm{VI}^{\mathrm{r}}_j = \frac{\boldsymbol{w}'^{\mathrm{r}}_j \boldsymbol{s}'^{\mathrm{r}}_j}{\left(\boldsymbol{f}'^{\mathrm{r}}_j\right)^2}. \tag{17}$$

Update left VI of right neighbours of $r_{\mathrm{max}i}$

$$\forall j \in \mathcal{N}^{\mathrm{r}}_{r_{\mathrm{max}i}}, \quad \mathrm{VI}^{\mathrm{l}}_j = \frac{\boldsymbol{w}'^{\mathrm{l}}_j \boldsymbol{s}'^{\mathrm{l}}_j}{\left(\boldsymbol{f}'^{\mathrm{l}}_j\right)^2}. \tag{18}$$

The updated values of MR and VI are plugged into the hypothesis tests defined in (4) and (5). Based on the outcome of these hypothesis tests, the CFAR method and corresponding neighbourhood are updated in accordance with the decision rule stated in Table 1. The neighbourhood set of every range cell is updated in accordance with (6) based on the updated values of MR and the outcome of hypothesis tests. At this step, the CFAR method employed in the previous stage is refined with reliable estimates of VI and MR. This enables to pick the most appropriate CFAR method for every range cell. The background sum vector and sample support vector are updated as shown in (19) to take into account for the updated neighbourhood set, $\mathcal{N}'^{\mathrm{S}}$

$$\begin{aligned} \boldsymbol{b}_j &= \sum_{k \in \mathcal{N}'^{\mathrm{S}}_j} x_k, \\ \boldsymbol{w}_j &= \left|\mathcal{N}'^{\mathrm{S}}_j\right|, \\ \boldsymbol{b}'_j &= \boldsymbol{b}_j, \\ \boldsymbol{w}'_j &= \boldsymbol{w}_j. \end{aligned} \tag{19}$$

After censoring all the outliers in the computation of VI and MR and altering the CFAR switch decisions and neighbourhood based on their new values, the background is recomputed to exclude these outliers. The censoring of an outlier in background estimation is performed on the full window or on the half window (left or right) based on the type of CFAR considered after decisions are refined.

- $\forall r_{\mathrm{max}i} \in \mathcal{M}_r$ and its guard cells (if considered) perform the following:

$$\forall j \in \mathcal{N}_{r_{\mathrm{max}i}}, \quad \text{if } r_{\mathrm{max}i} \in \mathcal{N}'^{\mathrm{S}}_j \text{ then}, \quad \boldsymbol{b}'_j = \boldsymbol{b}'_j - x_{r_{\mathrm{max}i}}. \tag{20}$$

Vector $\boldsymbol{b}'$ represents a modified background sum matrix after censoring.

The updated sample support vector is denoted as $\boldsymbol{w}'$. This is done to account for the reduction in sample support owing to rejection of outlier. This is shown in (21)

$$\forall j \in \mathcal{N}_{r_{\mathrm{max}i}}, \quad \text{if } r_{\mathrm{max}i} \in \mathcal{N}'^{\mathrm{S}}_j \text{ then}, \quad \boldsymbol{w}'_j = \boldsymbol{w}'_j - 1. \tag{21}$$

The RVI-CFAR derived here assumes two guard cells on either side of the test cell. In specific cases where the target return is limited to the test cell under consideration, the guard cells need not be considered and this further simplifies the implementation of RVI-CFAR. The modified final detection and outlier detection thresholds are recomputed using (9) and (10), respectively, by substituting modified background sum matrix $\boldsymbol{b}'$ to determine modified detection vectors $\boldsymbol{d}'^{\mathrm{D}}$ and $\boldsymbol{d}'^{\mathrm{O}}$.

The proposed RVI-CFAR detector does not require sorting operation to remove outliers in threshold computation and thus the detector is computationally efficient. The modified threshold vector enables the detection of new targets, which are otherwise obscured in the presence of strong interfering targets in their reference window. The detected range cells after the second stage of processing include the newly detected targets with the modified threshold vector and the detected targets from the first stage of processing. The outlier rejection stage of RVI-CFAR can be repeated to reject the newly detected targets from the second stage to recompute the modified threshold vector. This constitutes the third stage of processing (or the second pass of outlier rejection). The second pass of outlier rejection considers modified detection vector $\boldsymbol{d}'^{\mathrm{O}}$ instead of $\boldsymbol{d}^{\mathrm{O}}$ and all other original vectors. As described earlier, each stage of outlier rejection involves the exclusion of extraneous signal sample from background estimation, MR and VI statistics of affected range cells. This process of outlier rejection can be continued to the third pass taking the detection vector of the second pass. It is shown through simulations that three passes of outlier rejection are generally sufficient for detection of four to six closely spaced targets located anywhere in the reference window of the test cell. All the results obtained in this study use three or less number of passes of outlier rejection in the RVI-CFAR detector (alternatively four or less stages of processing inclusive of the first stage). If the number of targets detected at any stage is the same as the previous stage, censoring is terminated. The block diagram of the RVI-CFAR detector is shown in Fig. 1.

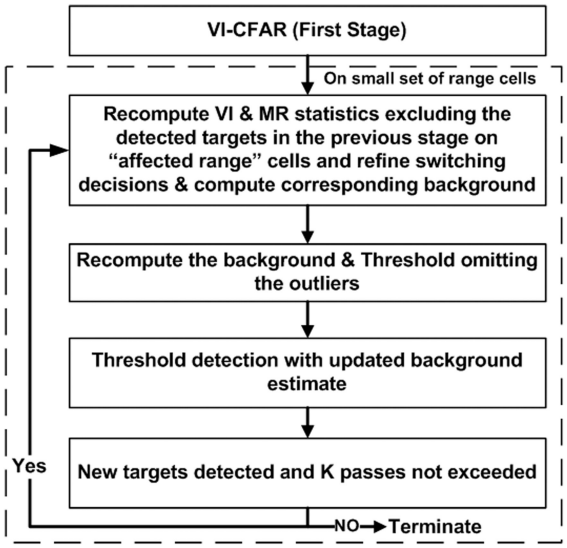

Fig. 1 *Block diagram of RVI-CFAR detector*

4 Performance analysis

4.1 Scope

The detector performance of CA, GO and SO CFAR methods in the presence of clutter edge and multiple interfering targets are studied in the literature. Analytical expressions for detection probability of primary target with multiple interfering targets in its reference window and the PFA at clutter edge are available in [5, 12]. However, the analysis provides expressions for detection probability of any target in the presence of multiple targets located in close proximity. If we consider the detection of a target as an event, such events are dependent events if the reference window of the target under consideration has other interfering targets. To analyse the performance parameters of RVI-CFAR, one requires determining the probability of detection of joint events, such as the probability of detection of at least one target or probability of detection of exactly two targets etc. This amounts to the determination of the joint distribution and this is complicated due to the interdependency of these events. Furthermore, the statistical nature of RVI-CFAR, which involves outlier rejection and CFAR switching based on hypothesis tests on VI and MR and lack of analytical characterisation of VI make the problem even more complex. Owing to these reasons, the evaluation of the proposed technique is carried out using Monte–Carlo simulations.

4.2 Simulation parameters

The proposed RVI-CFAR is evaluated for multiple interfering targets, clutter edge and when the reference window contains both clutter edge and interfering target scenarios. The performance is

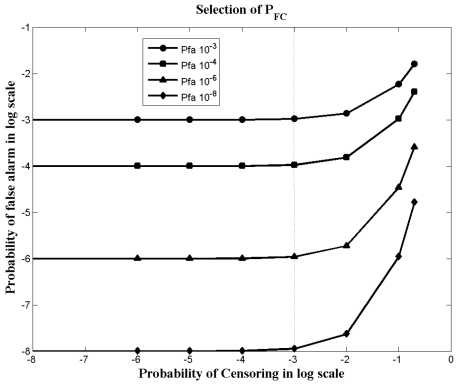

Fig. 2 *Selection of PFC for censoring*

compared with VI and OS and cell averaging (CA) CFAR detectors. To enable fair estimates of VI corresponding to right and left reference windows, a reference window size of 40 range cells is considered in the simulation. The PFA considered for most of the simulations is 1×10^{-4} or lesser. The performance of the RVI-CFAR detector in a multiple target environment is also studied and compared the OS CFAR detector for lower values of PFA of 1×10^{-6} and 1×10^{-8}. The SNR of the primary target is denoted by S, whereas the SNR of interfering targets is denoted by I. In all the simulations, the strength of the interfering target is considered relative to the strength of the primary target (I/S ratio). Both primary and interfering target returns are modelled by the 'Swerling-1' target fluctuation model. The 25th ordered sample is considered to be the background estimate in the case of OS CFAR. The threshold multiplier of OS CFAR corresponding to the 25th ordered sample is computed as given in [12].

The choice of PFC is discussed next assuming PFA of 1×10^{-4} or lesser. The dependency of $\bar{P}_{\mathrm{FA}}$ on $\bar{P}_{\mathrm{FC}}$ is brought out in Fig. 2. It is observed from the figure that, the choice of $\bar{P}_{\mathrm{FC}} > 1 \times 10^{-3}$ increases $\bar{P}_{\mathrm{FA}}$ to unacceptable levels. The use of higher $\bar{P}_{\mathrm{FC}}$ or equivalently lower outlier rejection threshold truncates the probability density function of noise samples due to the rejection of samples from the tail of the distribution (as an outlier in background estimation). As a result, the estimated noise power will be lesser than the actual noise power. This sets the detection threshold lower than required leading to an increased false alarm. It is evident from Fig. 2, an outlier detection threshold corresponding to $\bar{P}_{\mathrm{FC}}$ of 1×10^{-3} maintains the $\bar{P}_{\mathrm{FA}}$ at the design level for varying values of $\bar{P}_{\mathrm{FA}}$. Thus, $\bar{P}_{\mathrm{FA}} \leq \bar{P}_{\mathrm{FC}} \leq 1 \times 10^{-3}$ improves the performance of the detector without compromising on the number of false leaks. Thus, $\bar{P}_{\mathrm{FC}}$ is chosen to be equal to $\bar{P}_{\mathrm{FA}}$ in most of the simulations. Section 4.7 presents the results of RVI-CFAR detector with $\bar{P}_{\mathrm{FC}}$ set to 1×10^{-3}.

The threshold for hypothesis tests in VI-CFAR is chosen to control false alarm at the clutter edge and also handle non-homogeneity caused by the presence of secondary targets. The threshold K_{VI} is chosen to keep the classification error probability, β_0, low [25]. This probability is the probability of detecting non-homogeneity when the background is homogeneous. A high value of threshold K_{VI} keeps this error probability low. This is required to choose both the reference windows for background estimation under the homogeneous condition to minimise CFAR loss. However, there is a corresponding decrease in sensitivity to detect non-homogeneous conditions caused by interfering targets (discrete outliers). There is another consideration to be kept in mind while choosing the threshold for VI hypothesis test. The probability of choosing improper half window at the test cell with clutter power transition is also equal to classification probability error β_0. For a detector to have good performance at the clutter edges, it is required to keep this error probability low, in the same order of PFA. The resulting PFA at the clutter edge is approximately equal to $(1 + \beta_0/P_{\mathrm{FA,design}}) \times P_{\mathrm{FA,design}}$ [25]. In our simulations, the design PFA is kept at 1×10^{-4}. From simulations, it is found that the value of $K_{\mathrm{VI}} = 4$ corresponds to the error probability of 1.6×10^{-3}. For the value of $K_{\mathrm{VI}} = 4.0$, the resultant PFA would be 16 times of design PFA. The lower value of K_{MR} favours the use of GO-CFAR more often under homogeneous conditions and in an interfering target environment. This is undesirable due to the higher CFAR loss. The probability of detecting different means between left and right reference windows given that the background is homogeneous is denoted by γ_0 and this probability needs to be kept low. Higher value of K_{MR} keeps this probability low. However, at a test cell near a clutter edge, the means of both left and right reference windows look alike, as a few clutter samples dominate the remaining noise samples in one half of the reference window, while the other contains samples from higher clutter background. A higher value of γ_0 (or lower value of K_{MR}) favours the selection of proper window to reduce false leaks near the vicinity of a clutter transition. This is called secondary false alarm probability. In our simulation, value of 2 is chosen to keep γ_0 at 0.03 in the evaluation of RVI-CFAR.

The performance of the proposed RVI-CFAR detector is evaluated using a maximum of three passes of outlier rejection. The simulation results are obtained using 10,000 Monte–Carlo trials to arrive at detection probability versus SNR curves for both homogeneous and non-homogeneous cases. A multiple target environment with two, three and four close by targets is considered for evaluation. The location of interfering targets is not constrained to any one side of the test cell. The interfering targets are considered to be at random locations in the reference window on either side of the test cell. The performance of the VI-CFAR detector severely gets degraded in the event of the interfering targets located on both sides of the test cell (i.e. in both right and left reference windows). The analysis is also carried out to estimate the average number of censoring steps required for multiple target scenarios along with window selection probability. Furthermore, the performance is presented when the reference window contains both interfering targets and the clutter edge. Initially, the test cell and interfering targets are considered in the clear region with a clutter-to-noise ratio (CNR) of 20 dB for the clutter edge. In the second case, all the targets are considered in the clutter region. We further present the simulation results to show the invariance of VI (at the cell under test) for multiple targets scenario in case of RVI-CFAR. The performance of the proposed detector is also evaluated for a clutter edge scenario with a CNR of 20 dB and the PFA is obtained using 1,000,000 Monte–Carlo trials.

4.3 Homogeneous background

Fig. 3 shows the probability of detection of RVI-CFAR in comparison with CA, OS, VI and ideal detector for the homogeneous background. The detection performance of all the CFAR detectors is similar. However, all the CFAR processors show CFAR loss in comparison with a detector with known interference power.

4.4 Multiple target environment

A multiple target scenario is considered and the detection performance (of the primary target) of RVI-CFAR is compared to OS, VI CFAR detectors and is shown in Fig. 4. Three interfering targets, located on one side of the test cell, are considered for evaluation. The locations of all three interfering targets are considered to the left of the primary target. Then, $I/S = 1$ is considered. Fig. 5 shows the probability of window selection in RVI and VI-CFAR detectors for background estimation at the test cell location. As could be noticed, the proposed RVI-CFAR employs both the reference windows (both left and right windows) for background estimation, unlike VI-CFAR. VI-CFAR selects the right reference window for background estimation. The RVI-CFAR detector selects the largest available sample support excluding the outliers and thus does not suffer from additional CFAR loss compared to VI-CFAR. The performance of RVI-CFAR has no significant loss compared to OS-CFAR. The detection performance of RVI-CFAR is 0.5 dB better than VI-CFAR at a SNR value of 10 dB. The gain in detection performance is computed as the

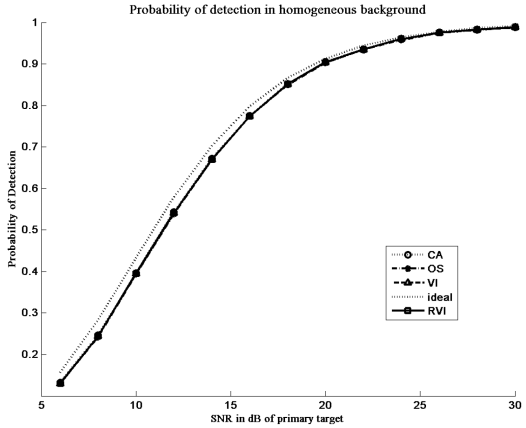

Fig. 3 *Comparison of detection probability of RVI-CFAR, VI-CFAR, and OS-CFAR for homogeneous background*

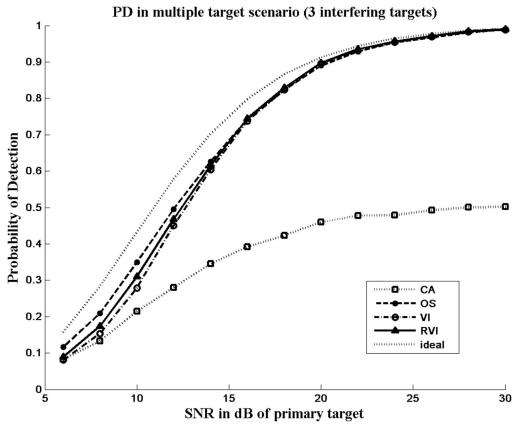

Fig. 4 *Comparison of detection probability of RVI-CFAR, VI-CFAR, and OS-CFAR with three interfering targets located on one side of the test cell with* $I/S = 1$

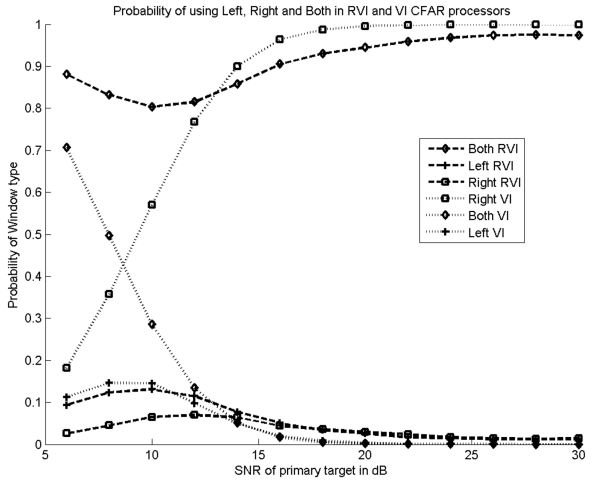

Fig. 5 *Window selection for three interfering targets located on one side of the test cell for RVI-CFAR and VI CFAR*

difference in SNR between RVI-CFAR and VI-CFAR detectors at a given probability of detection.

Another multiple target scenario with four interfering targets, distributed on either side of the test cell, is considered and the results are shown in Fig. 6. Then, $I/S = 1$ is considered. The performance of RVI-CFAR is similar to OS-CFAR. However, VI CFAR suffers unacceptable degradation in detection probability of the target in the test cell. The reference window considered in RVI-CFAR is shown in Fig. 7 at the test cell location and it is evident that the RVI-CFAR uses both the reference windows most of the time, thus minimises the CFAR loss. Next, the detection performance of RVI-CFAR detector in a multiple target

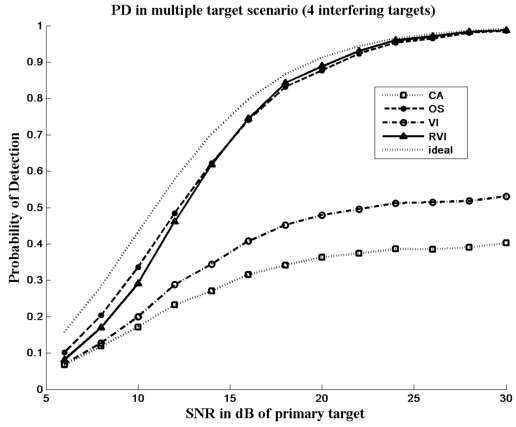

Fig. 6 *Comparison of detection probability of RVI-CFAR, VI-CFAR, and OS-CFAR for four interfering targets located on both sides of the test cell with* $I/S = 1$

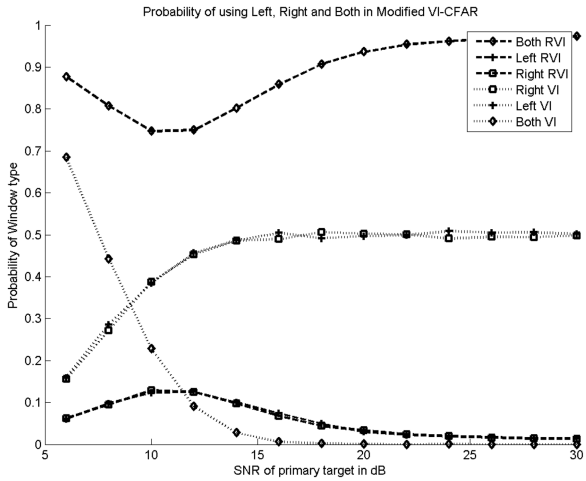

Fig. 7 *Window selection for four interfering targets located on both sides of the test cell for RVI-CFAR and VI-CFAR*

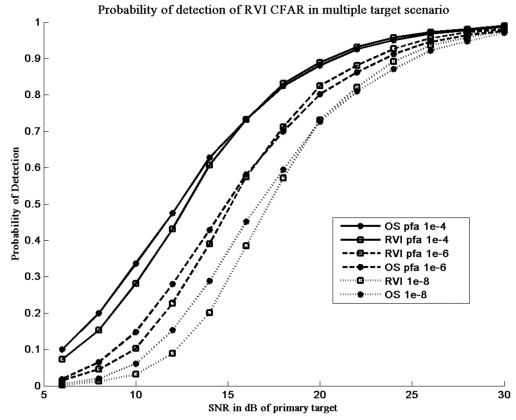

Fig. 8 *Performance of RVI-CFAR for varying PFA*

environment with four targets distributed on either side of the test cell is considered for varying PFA and is compared with OS-CFAR. The results are presented in Fig. 8. It is evident that the performance of the proposed RVI-CFAR is very closely comparable to OS-CFAR for all the cases of the PFA considered in this simulation. In all the multiple target scenarios, the detection performance of CA-CFAR is unacceptably degraded due to the masking effect of the primary target.

The average number of outlier rejection stages (passes) required is around 1.2–2.5 for the cases of 3–9 interfering targets and it is shown in Fig. 9 as a function of the SNR of the primary target. Then, $I/S = 1$ is considered for this simulation.

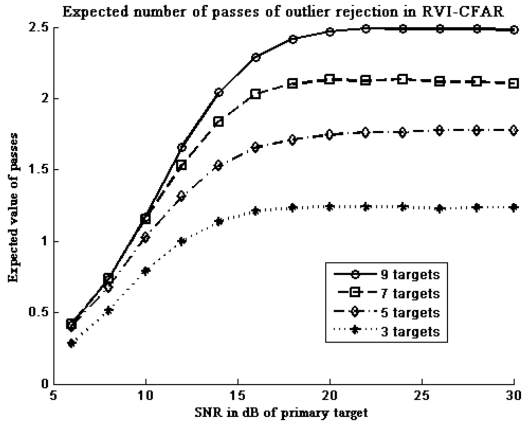

Fig. 9 *Expected number of censoring stages required in different multiple target environments in RVI-CFAR*

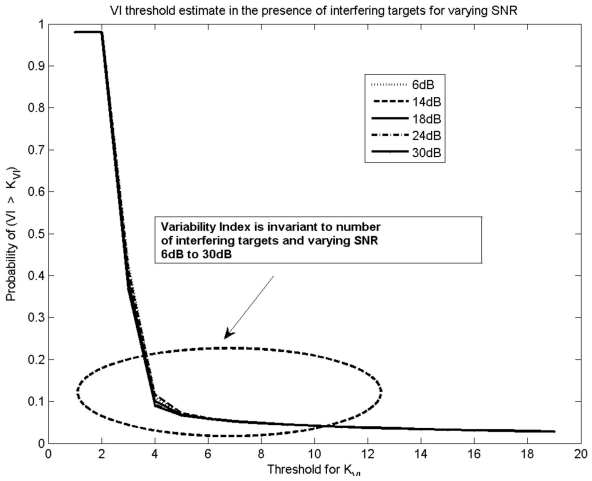

Fig. 10 *Probability of variable hypothesis decision as a function of threshold K_{VI} in the presence of three interfering targets*

Since RVI-CFAR removes outliers in the computation of VI and MR, the VI is independent of the number of interfering targets present and their SNR. This allows RVI-CFAR to choose samples from both left and right reference windows for background estimation under non-homogeneous conditions caused by multiple interfering targets. The plot of VI is shown in Fig. 10. However, in VI-CFAR, the VI varies in the presence of interfering targets (see Figs. 2 and 3 of [25]) and this information is used to select the reference window [25]. The invariance of VI in the presence of multiple interfering targets is an important feature of RVI-CFAR and this ensures the selection of optimum sample support in multiple target scenarios, thereby minimising the CFAR loss incurred. The other advantage of invariance of VI is in regulating the false leaks at the clutter edge in the presence of targets in the vicinity of clutter transition. In VI-CFAR, the presence of multiple targets near a clutter edge contaminates the VI and leads to improper selection of a reference window. The presence of targets in the clutter region disturbs the VI and leads to the selection of improper lower power reference window and thereby allowing intolerable levels of false leaks. On the other hand, the presence of targets in a clear region near a clutter edge regulates the false leaks but suffers from degraded detection performance. These effects are undesirable. This problem does not exist in RVI-CFAR.

4.5 Clutter edge

Fig. 11 shows the PFA for the test cell at the clutter edge with a CNR of 20 dB. The threshold values of VI and MR used in the simulation are $K_{\mathrm{VI}} = 4.0$ and $K_{\mathrm{MR}} = 2.0$, respectively. A single clutter transition from low to high, when traversed from left to right with CNR of 20 dB, is simulated. The clutter edge is simulated at the range cell number 100. It can be concluded that the

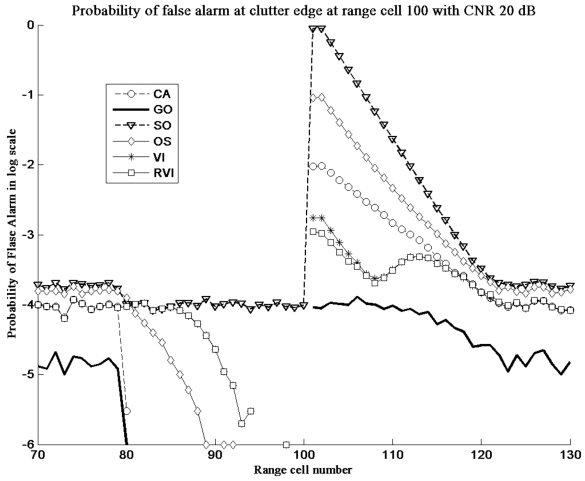

Fig. 11 *PFA at clutter transition range cell for RVI-CFAR, CA-CFAR, SO-CFAR, GO-CFAR, VI-CFAR, and OS-CFAR with a CNR of 20 dB*

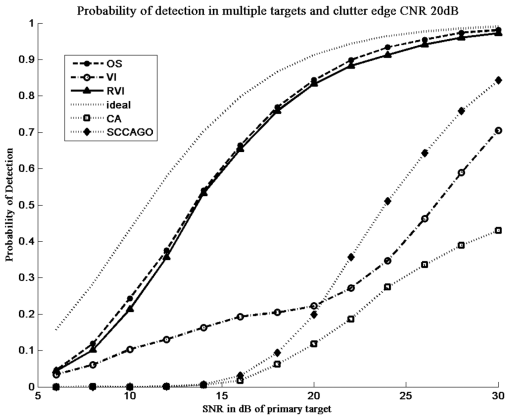

Fig. 12 *Detection probability of primary target in clear region with three interfering targets also in the clear region and clutter edge of CNR 20 dB*

RVI-CFAR exhibits detection performance comparable to OS-CFAR with better regulation of false leaks.

4.6 Clutter edge and multiple target scenario

The detection performance of the primary target in the presence of interfering targets and clutter edge is shown in Fig. 12. Three interfering targets are located to the left of the primary target in the clear region. Then, $I/S = 1$ is considered for simulating interfering targets. The primary target is also considered in the clear region. The clutter edge is to the right of the test cell and fills up five samples in the reference window. The detection performance is obtained for K_{VI} threshold value of 4.0 and K_{MR} value of 2.0. The CNR of the clutter edge is 20 dB. The probability of window selection for this scenario at the test cell location is shown in Fig. 13. It is noticed that the RVI-CFAR uses the left window of the primary target to estimate the background. The performance of RVI-CFAR is close to OS CFAR with better control on false leaks. VI-CFAR suffers greater performance loss due to the reasons explained earlier. The SCCAGO-CFAR and CA-CFAR detectors also suffer performance loss for this scenario, as they consider both the reference windows for background estimation.

In the next scenario, the primary target is considered in the clutter region along with three interfering targets to its right in the clutter region. The clutter transition is to the left of the primary target and CNR considered is 10 dB. The detection performance is shown in Fig. 14. A loss of 1.5 dB is observed in the detection performance of RVI-CFAR compared to OS-CFAR. This loss is computed as the additional SNR required in RVI-CFAR detector compared to OS-CFAR to achieve the probability of detection of 0.3 in both the detectors. VI-CFAR performs marginally better than RVI-CFAR. The detection performance of SCCAGO-CFAR and RVI-CFAR is almost identical for this case. CA-CFAR suffers from

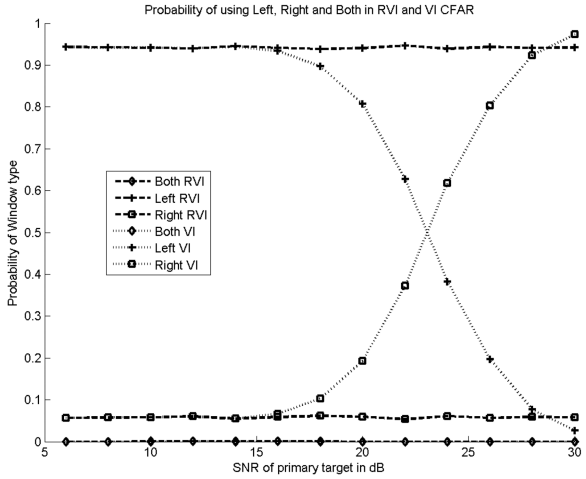

Fig. 13 *Window selection for the case of clutter edge on the right side and three interfering targets on the left side of the primary target*

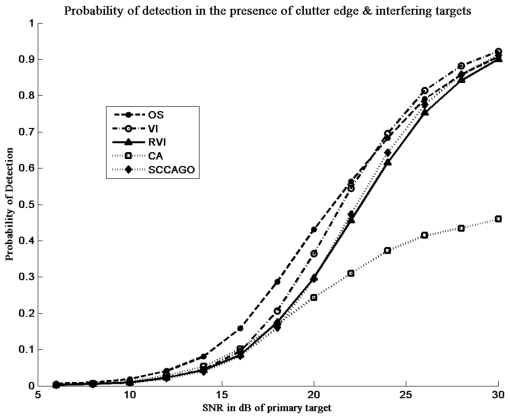

Fig. 14 *Probability of Detection (PD) of the primary target in clutter region with three interfering targets also in clutter region and clutter edge of CNR 10 dB*

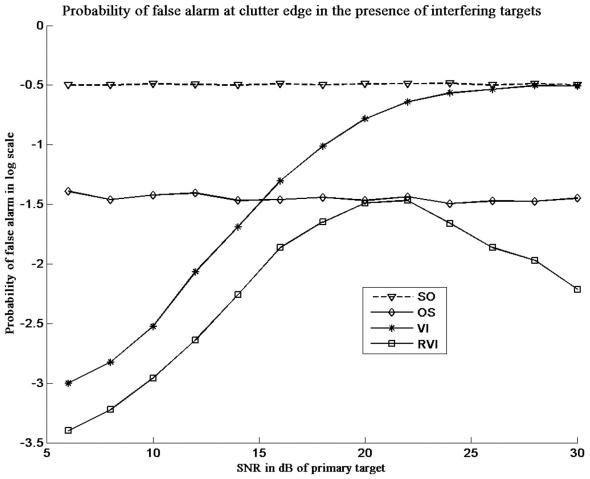

Fig. 15 *PFA at clutter edge with four targets in clutter region and clutter edge of CNR 10 dB*

performance loss due to the presence of interfering targets in the reference window of the test cell from the clutter region. However, the false alarm regulation of OS, VI, SCCAGO, and CA-CFAR methods are inferior to RVI-CFAR. Fig. 15 shows the PFA at the test cell with clutter transition when four targets are present in its reference window in the clutter region. It is observed that the PFA of OS CFAR is higher, whereas RVI-CFAR exhibits better regulation of false leaks except when the resultant SNR of interfering targets (SNR with respect to changed background power) is close to the CNR of clutter edge. VI-CFAR fails to

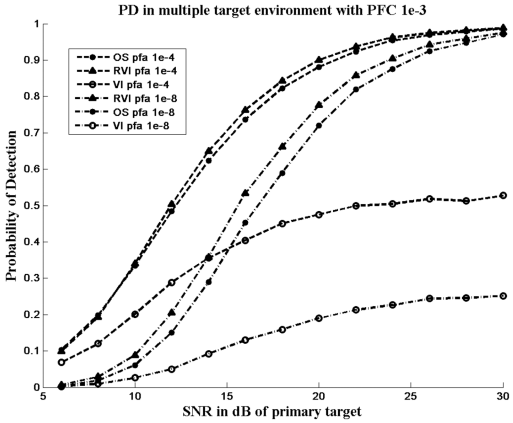

Fig. 16 *PD comparison of RVI-CFAR, OS CFAR, VI CFAR for four interfering targets on both sides with $I/S = 1$, PFC 1×10^{-3} and PFA of 1×10^{-4} and 1×10^{-8}*

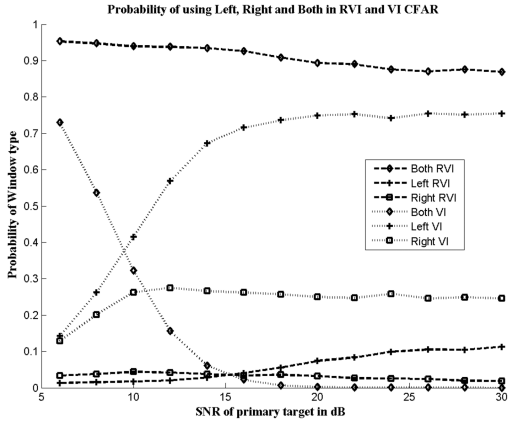

Fig. 17 *Probability of using reference window options in RVI and VI CFAR detectors for four interfering targets on both sides with $I/S = 1$ and lower outlier detection threshold and design PFA of 1×10^{-4}*

contain false leaks in the higher SNR region of the interfering targets.

4.7 Performance of RVI-CFAR for higher PFC

The performance of RVI-CFAR is evaluated in a multiple target environment, considering the outlier detection threshold corresponding to PFC of 1×10^{-3}. Four interfering targets, located on either side of the primary target, are considered with $I/S = 1$. Fig. 16 shows the performance of the RVI-CFAR detector in comparison with OS-CFAR for the case of detection threshold corresponding to PFA of 1×10^{-4} and 1×10^{-8}. The RVI-CFAR detector outperforms OS-CFAR in the high-SNR region by 0.5 dB for the case of 1×10^{-4}, while its performance is marginally better in the low-SNR region. For the case of 1×10^{-8} its performance is better by 1 dB compared to OS-CFAR. It can be recalled that there was a loss observed in the RVI-CFAR detector in comparison with OS-CFAR for this scenario in the low-SNR region, with the outlier detection threshold set equal to the detection threshold. The reference window used in RVI-CFAR for background estimation for this scenario is shown in Fig. 17 and it is observed that the probability of using both the reference windows (maximum sample support) is larger than that of RVI-CFAR with outlier detection threshold set equal to the detection threshold. This helps in minimising CFAR loss. Next, we consider the performance of RVI-CFAR at clutter edge with a CNR of 20 dB and it is shown in Fig. 18. It can be observed that the lower outlier detection threshold does not have an adverse impact on the performance of RVI-CFAR detectors at the clutter edge.

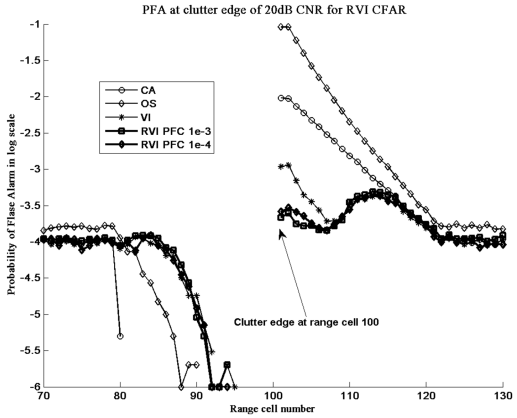

Fig. 18 *PFA at clutter edge for RVI-CFAR, RVI-CFAR, CA-CFAR, OS-CFAR, and VI-CFAR with a CNR of 20 dB with lower outlier detection threshold and design PFA of* 1×10^{-4}

5 Conclusion

The proposed RVI-CFAR detector does not rely on the sorting operation to reject outliers and thus computationally efficient compared to censored CFAR detectors requiring ranking like OS-CFAR. Furthermore, OS-CFAR requires prior knowledge of the number of interfering targets in the reference window to decide the depth of censoring, whereas the proposed techniques do not require this information for outlier rejection. The location of interfering targets is not restricted to a single side of the cell under test in the case of RVI-CFAR to achieve similar performance compared to OS-CFAR. This is not so for VI-CFAR. The proposed RVI-CFAR exhibits improved performance in all cases of interfering target scenarios compared to VI-CFAR. The first stage of processing involves outlier identification or detection of strong targets by VI-CFAR. This is followed by censoring of outliers in the computation of background estimate, MR and VI of affected range cells, which are the detected range cells and their neighbours. Thus, the outlier rejection stages of RVI-CFAR operate on a small set of range cells. The operations involved in censoring of outliers are mostly matrix operations facilitating efficient implementation on hardware accelerators. The proposed approach requires only first- and second-order moments to be computed to identify and reject outliers. Besides this, the approach makes no assumption on the maximum level of background power and thus fully adaptive, unlike excision CFAR.

RVI-CFAR provides an efficient solution to a challenging scenario, wherein the reference window contains both clutter edge and interfering targets. The detection performance is evaluated when all the targets are in the clear region and the reference window contains a few samples from the clutter region. Simulation studies show that the performance of RVI-CFAR is better than VI-CFAR and comparable to OS CFAR and meanwhile maintains false leaks significantly lower than OS CFAR at the clutter edge. RVI-CFAR shows a loss of 1.5 dB OS CFAR when targets are present in the clutter region. However, RVI-CFAR exhibits better control on false leaks compared to OS and VI CFAR, except in the critical region. When the resultant SNR of targets in clutter region is close to CNR of the clutter edge, the false alarm of RVI-CFAR is close to OS CFAR. It is concluded that the performance RVI-CFAR is comparable to OS CFAR for all the interference scenarios with better regulation properties of false leaks at the clutter edge. Furthermore, the detection performance of RVI-CFAR is close to optimum CA-CFAR for the homogeneous background. The use of a higher PFC improves the detection performance of the proposed RVI-CFAR in multiple target scenarios at the cost of marginally higher computational requirement. It is observed that the performance of RVI-CFAR outperforms OS-CFAR even in a low-SNR region with the use of lower outlier identification threshold than the detection threshold.

6 References

[1] Finn, H.M., Johnson, R.S.: 'Adaptive detection mode with threshold control as a function of spatially sampled clutter level estimates', *RCA Rev.*, 1968, **29**, pp. 414–464

[2] Trunk, G.V.: 'Range resolution of targets using automatic detectors', *IEEE Trans. Aerosp. Electron. Syst.*, 1978, **AES-14**, (5), pp. 750–755

[3] Hansen, V.G., Sawyers, J.H.: 'Detectability loss due to 'greatest of' selection in a cell-averaging CFAR', *IEEE Trans. Aerosp. Electron. Syst.*, 1980, **AES-16**, (1), pp. 115–118

[4] Hansen, V.G.: 'Constant false alarm rate processing in search radars'. Proc. IEEE 1973 Int. Radar Conf., London, 1973, pp. 325–332

[5] Weiss, M.: 'Analysis of some modified cell-averaging CFAR processors in multiple-target situations', *IEEE Trans. Aerosp. Electron. Syst.*, 1982, **AES-18**, (1), pp. 102–114

[6] Zhang, Y., Gao, M., Li, Y.: 'Performance analysis of typical mean-level CFAR detectors in the interfering target background'. 2014 9th IEEE Conf. on Industrial Electronics and Applications, Hangzhou, China, June 2014, pp. 1045–1048

[7] Barboy, B., Lomes, A., Perkalski, E.: 'Cell-averaging CFAR for multiple-target situations', *IEE Proc. F, Commun. Radar Signal Process.*, 1986, **133**, (2), pp. 176–186

[8] Cui, Y., Zhou, G., Yang, J., *et al.*: 'On the iterative censoring for target detection in SAR images', *IEEE Geosci. Remote Sens. Lett.*, 2011, **8**, (4), pp. 641–645

[9] Gao, G., Liu, L., Zhao, L., *et al.*: 'An adaptive and fast CFAR algorithm based on automatic censoring for target detection in high-resolution SAR images', *IEEE Trans. Geosci. Remote Sens.*, 2009, **47**, (6), pp. 1685–1697

[10] Narasimhan, R.S., Vengadarajan, A., Ramakrishnan, K.R.: 'Design and efficient implementation of censored cell averaging CFAR for non-homogeneous background'. 2018 IEEE Aerospace Conf., Big Sky, MT, USA, March 2018, pp. 1–12

[11] Rohling, H.: 'Radar CFAR thresholding in clutter and multiple target situations', *IEEE Trans. Aerosp. Electron. Syst.*, 1983, **AES-19**, (4), pp. 608–621

[12] Gandhi, P.P., Kassam, S.A.: 'Analysis of CFAR processors in nonhomogeneous background', *IEEE Trans. Aerosp. Electron. Syst.*, 1988, **24**, (4), pp. 427–445

[13] Tom, A., Viswanathan, R.: 'Switched order statistics CFAR test for target detection'. 2008 IEEE Radar Conf., Rome, Italy, May 2008, pp. 1–5

[14] Ritcey, J.A.: 'Performance analysis of the censored mean-level detector', *IEEE Trans. Aerosp. Electron. Syst.*, 1986, **AES-22**, (4), pp. 443–454

[15] Rickard, J.T., Dillard, G.M.: 'Adaptive detection algorithms for multiple-target situations', *IEEE Trans. Aerosp. Electron. Syst.*, 1977, **AES-13**, (4), pp. 338–343

[16] Barkat, M., Himonas, S.D., Varshney, P.K.: 'CFAR detection for multiple target situations', *IEE Proc. F, Radar Signal Process.*, 1989, **136**, (5), pp. 193–209

[17] El Mashade, M.B.: 'Analysis of the censored-mean level CFAR processor in multiple target and nonuniform clutter', *IEE Proc., Radar Sonar Navig.*, 1995, **142**, (5), pp. 259–266

[18] Himonas, S.D.: 'A robust automatic censored CFAR detector for nonhomogeneous environments'. Proc. 1991 IEEE National Radar Conf., Los Angeles, CA, USA, March 1991, pp. 117–121

[19] Himonas, S.D.: 'Adaptive censored greatest-of CFAR detection', *IEE Proc. F, Radar Signal Process.*, 1992, **139**, (3), pp. 247–255

[20] Himonas, S.D., Barkat, M.: 'Automatic censored CFAR detection for nonhomogeneous environments', *IEEE Trans. Aerosp. Electron. Syst.*, 1992, **28**, (1), pp. 286–304

[21] Prastitis, L.A., Frank, J., Himonas, S.D.: 'Automatic censored cell averaging CFAR detector in nonhomogeneous clutter'. 1992 Int. Conf. on Radar, Brighton, UK, October 1992, pp. 218–221

[22] Tao, D., Anfinsen, S.N., Brekke, C.: 'Robust CFAR detector based on truncated statistics in multiple-target situations', *IEEE Trans. Geosci. Remote Sens.*, 2016, **54**, (1), pp. 117–134

[23] El Mashade, M.B.: 'Heterogeneous performance evaluation of sophisticated versions of CFAR detection schemes', *Radioelectron. Commun. Syst.*, 2016, **59**, (12), pp. 536–551. doi:

[24] Li, X., Zhang, Y., Pei, B.: 'An improved nonparametric detector for nonhomogeneous clutter environment'. 2014 IEEE Symp. on Computer Applications and Communications, Weihai, China, July 2014, pp. 10–13

[25] Smith, M.E., Varshney, P.K.: 'Intelligent CFAR processor based on data variability', *IEEE Trans. Aerosp. Electron. Syst.*, 2000, **36**, (3), pp. 837–847

[26] Patel, V., Madhukar, H., Ravichandran, S.: 'Variability index constant false alarm rate for marine target detection'. 2018 Conf. on Signal Processing And Communication Engineering Systems (SPACES), Vijayawada, India, January 2018, pp. 171–175

[27] Cheikh, K., Soltani, F.: 'Performance of the fuzzy VI-CFAR detector in non-homogeneous environments'. 2011 IEEE Int. Conf. on Signal and Image Processing Applications (ICSIPA), Kuala Lumpur, Malaysia, November 2011, pp. 100–103

[28] Farrouki, A., Barkat, M.: 'Automatic censoring CFAR detector based on ordered data variability for nonhomogeneous environments', *IEE Proc., Radar Sonar Navig.*, 2005, **152**, (1), pp. 43–51

[29] Zhao, J., Tao, R., Wang, Y.: 'A new CFAR detector based on ordered data variability'. First Int. Conf. on Innovative Computing, Information and Control – Volume I (ICICIC'06), Beijing, China, August 2006, vol. 2, pp. 628–631

[30] Hu, W., Wang, Y., Wang, S., *et al.*: 'A robust CFAR detector based on ordered statistic'. 2006 CIE Int. Conf. on Radar, Shanghai, China, October 2006, pp. 1–4

[31] Ran, S., Zhao, H., Fu, Q.: 'An adaptive CFAR detector for range-spread target in various environments'. 2012 IEEE 11th Int. Conf. on Signal Processing, Beijing, China, October 2012, vol. 3, pp. 1980–1983
[32] Xu, C., He, Y., Yao, Q., *et al.*: 'A modified robust CFAR detector'. Proc. 2011 Int. Conf. on Electronic Mechanical Engineering and Information Technology, Harbin, China, August 2011, vol. 9, pp. 4439–4442
[33] Zhang, R., Zou, Y., Sheng, W., *et al.*: 'An improved CFAR detector for nonhomogeneous clutter environment'. 2010 Int. Symp. on Signals, Systems and Electronics, Nanjing, China, September 2010, vol. 2, pp. 1–4
[34] Zaimbashi, A., Norouzi, Y.: 'A robust CFAR detector in non-homogenous environment'. 2008 IEEE Radar Conf., Rome, Italy, May 2008, pp. 1–4
[35] Rohman, B.P.A., Kurniawan, D., Miftahushudur, M.T.: 'Switching CA/OS CFAR using neural network for radar target detection in non-homogeneous environment'. 2015 Int. Electronics Symp. (IES), Surabaya, Indonesia, September 2015, pp. 280–283
[36] Zhou, W., Xie, J., Xi, K., *et al.*: 'Modified cell averaging CFAR detector based on Grubbs criterion in non-homogeneous background', *IET Radar Sonar Navig.*, 2019, **13**, (1), pp. 104–112
[37] Rohatgi, V.K., Ehsanes Saleh, A.K.M.: '*An introduction to probability and statistics*' (Wiley-Blackwell, NY, USA, 2011, 2nd edn.)
[38] Richards, M.: '*Fundamentals of radar signal processing*' (McGraw Hill Education Private Limited, NY, USA, 2005)